Special Section: Erosion and Lateral Surface Processes

Core Ideas

- Discharge and sediment concentrations were measured in a drained catchment.
- The impact of tile drainage at the catchment scale was analyzed with a nested approach.
- The major part of sediment fluxes occurred during winter floods.
- Sediment transfer in the tile drain was episodic although significant.

T. Grangeon, L. Manière, A. Foucher, I. Pene-Galland, and S. Salvador-Blanes, E.A. 6293, GéoHydrosystèmes Continentaux (GéHCO), Univ. François Rabelais de Tours, Faculté des Sciences et Techniques, Tours, France; T. Grangeon, R. Vandromme, and O. Cerdan, Dép. Risques et Prévention, Bureau de Recherches Géologiques et Minières, Orléans, France; O. Evrard, Lab. des Sciences et de l'Environnement, UMR 8212 (CEA/CNRS/UVSQ), Univ. Paris-Saclay, Domaine du CNRS, Gif-sur-Yvette, France. *Corresponding author: (thomas.grangeon@univ-tours.fr; o.cerdan@brgm.fr).

Received 31 May 2017.
Accepted 25 Aug. 2017.

Citation: Grangeon, T., L. Manière, A. Foucher, R. Vandromme, O. Cerdan, O. Evrard, I. Pene-Galland, and S. Salvador-Blanes. 2017. Hydro-sedimentary dynamics of a drained agricultural headwater catchment: a nested monitoring approach. Vadose Zone J. 16(12). doi:10.2136/vzj2017.05.0113

Hydro-sedimentary Dynamics of a Drained Agricultural Headwater Catchment: A Nested Monitoring Approach

T. Grangeon,* L. Manière, A. Foucher, R. Vandromme, O. Cerdan,* O. Evrard, I. Pene-Galland, and S. Salvador-Blanes

Soil erosion and sediment transfer are extensive in lowland agricultural catchments. In these environments, high-frequency datasets of both water discharge and suspended sediment concentrations are often lacking. In particular, the impact of tile drainage networks on sediment fluxes in these catchments is poorly understood. Our research quantified sediment fluxes between 2013 and 2016 at five nested stations including a tile drain outlet across a small (25-km^2) agricultural catchment (Loire River basin, France) representative of lowland cultivated environments of the middle part of this basin. Sediment fluxes varied from 1 to 38 t km^{-2} yr^{-1} across the monitored subcatchments. Most of sediment fluxes (79 ± 9%) were measured during flood events (n = 44), mostly occurring in winter (75%) and spring (20%). Seasonality controlled most of the variations of sediment fluxes. Sediment transfers in tile drains occurred episodically. Flows were measured during 11.4% of the monitoring time. A mean time lag of 80 min was recorded between the peak discharge at the drain outlet and the downstream river station. At the event scale, sediment fluxes exported from the tile drain varied between 1.1×10^{-4} and 2.5 t km^{-2} and remained on the same order of magnitude as those measured at the downstream river station, although the latter were on average 53% lower. Results suggest significant storage of sediment materials in the river channel and their export during the most intense flood events. Our research emphasizes the need for continuous monitoring of water and sediment transfers in agricultural catchments equipped with tile drains.

Important soil erosion leads to numerous on-site impacts, and it may also supply large quantities of fine particles to rivers. When excessive sediment loads are delivered to the river, they are associated with detrimental environmental impacts (Owens et al., 2005) through the increase of turbidity within the water column and river bed clogging (Kemp et al., 2011; Kjelland et al., 2015). Accordingly, a better understanding of the processes controlling sediment transfer is needed to design efficient mitigation strategies.

The main processes controlling soil erosion on hillslopes have long been studied (e.g., Bradford et al., 1987; Le Bissonnais and Singer, 1992), and their global mechanisms are now reasonably known (Kinnell, 2005), although work remains to be done to understand erosion at various scales (Auerswald et al., 2009; García-Ruiz et al., 2013). These previous research efforts demonstrated that soil erosion is the result of rainfall and overland flow detachment and transport (e.g., Hairsine and Rose, 1992). These conceptual and modeling frameworks are largely used in current sediment simulation modeling studies (Nord and Esteves 2005; Jomaa et al., 2010; Cea et al., 2016). However, the spatial and temporal dynamics of sediment fluxes must be further measured and analyzed to improve our understanding of the possible connections and disconnections between the water and sediment transport pathways, which largely control sediment transfer at the catchment scale (Wainwright et al., 2008; López-Vicente et al., 2015; Parsons et al., 2015).

Although suspended sediment yield was shown to globally decrease with slope (Milliman and Syvitski, 1992), small headwater lowland catchments may exhibit significant sediment exports (Vanmaercke et al., 2011). Previous studies investigated sediment transfer in these catchments by sediment budget (Walling and Collins, 2008) or sediment fingerprinting (Smith and Blake, 2014; Foucher et al., 2015; Le Gall et al., 2017) approaches. Russell et al. (2001) and Walling et al. (2002) demonstrated the need to take into account tile drain networks in lowland catchments equipped with these systems. Although tile drains increase water and sediment connectivity across catchments, they are generally not taken into account in models simulating soil erosion and sediment transfers. This lack is probably associated with the current poor understanding of tile drain behavior. Although progress has been made to characterize water and dissolved matter transfers through tile drains (e.g., Ulén and Persson, 1999; Macrae et al., 2007; Rozemeijer et al., 2010; Li et al., 2010), sediment transport in these systems has rarely been quantified (Turtola et al., 2007; Bilotta et al., 2008), and the few studies that achieved this goal were conducted at the plot scale. The upscaling of these results from the field to the catchment scale is not straightforward (de Vente and Poesen, 2005; Delmas et al., 2012).

To the best of our knowledge, sediment dynamics in an agricultural drained catchment has never been measured with a high frequency. Indeed, because it has been shown that sediment transfers in headwater catchments occur during very short time periods (Meybeck et al., 2003), high temporal resolution monitoring (<1 h) is required to capture the temporal variations of these sediment fluxes, as was previously done for water fluxes in drained cultivated environments (King et al., 2014; Muma et al., 2016). As these previous studies demonstrated the increased connectivity associated with tile drainage networks for water transfers, a similar investigation should be conducted on sediment transfers. It is therefore important to combine stations monitoring sediment transport at both tile drain outlets and in rivers.

Accordingly, the goal of this research was to measure water and sediment fluxes with a high spatial (5.1×10^{-2} to 6 km^2) and temporal (15 min) resolution and to characterize the hydro-sedimentary behavior of a small (25-km^2) tile-drained agricultural catchment (Louroux River, France) representative of those found in similar environments of the Loire River basin, with a specific emphasis on tile drain dynamics. To this end, a nested approach was adopted, including measurements from the individual tile-drained field to the catchment outlet, providing a unique dataset and new insights into the sediment dynamics of small headwater agricultural catchments.

Materials and Methods

Louroux Catchment

The Louroux catchment is located in the center of France (250 km southwest of Paris; Fig. 1). It is a 25-km^2 agricultural lowland catchment located within the Loire River basin. The lithology consists of post-Helvetian sand and continental gravels (32%), Senonian flint clays (23%), Quaternary loess (18%), Helvetian shelly sands (18%), Ludian Touraine lacustrine limestones (6%), and Eocene silicic conglomerate (2%) (Rasplus et al., 1982). The main soil types are: Neoluvisols, Brunisols, Calcosols, and Calcisols. The catchment is mainly occupied by arable land (78%), forest (15%), and grassland (7%). Wheat (*Triticum aestivum* L.), sunflower (*Helianthus annuus* L.), and maize (*Zea mays* L.) are the main crops cultivated in the region. In the Louroux catchment, they represent >67% of the cultivated fields. An airborne lidar digital elevation model at a 1-m resolution was used to characterize the main topographical features of the catchment.

The catchment is characterized by very low slope gradients (the mode of the slope statistical distribution is 1.2%) and is drained by a dense network of ditches (Table 1). The water flow pathways were derived through the combination of lidar data, field observations, and aerial photographs to take into account local obstacles and the flow of ditches through culverts across roads. Most of the fields are equipped with tile drains.

The climate is temperate oceanic, with mean monthly temperatures ranging from 2 to 24°C. The mean annual rainfall is 684 mm at the nearby Tours station according to the national weather service based on records from 1981 to 2010. By comparison with the mean altitude, annual rainfall, and drainage area of the Loire River basin catchments, the Louroux catchment is representative of environments found in the middle part of this basin (Gay et al., 2014); 60, 25, and 20% of the 110 measured catchments had a mean altitude, a mean annual rainfall, and a drained area, respectively, comparable to the ones calculated for the Louroux catchment.

Hydrological Monitoring Stations

Five monitoring stations were used to quantify water and sediment fluxes across the main Louroux subcatchments (Fig. 2). One station measured the fluxes from an individual tile drain outlet (Brépinière) draining a surface area of 5.1×10^{-2} km^{-2}. It is embedded in one of the monitored subcatchments (Masniers). Because of probe failures and a high level of noise in the recorded data, one of the monitored catchments (Picarderie) was removed from further analysis. The data recorded from four river stations and the tile drain outlet were analyzed for a period of three hydrological years, covering September 2013 to August 2016.

Each monitoring station was equipped with an OTT PLS (pressure level sensor) water level probe. Discharge was derived from the water level using rating curves obtained through gauging during both flood events and base flow periods. Three stations were equipped with a calibrated flume, which allows a direct estimation of discharge for low to moderate flows. During the largest flood events, when an overflow occurred in the flumes, gauging was performed to extrapolate the rating curve for these high flow values.

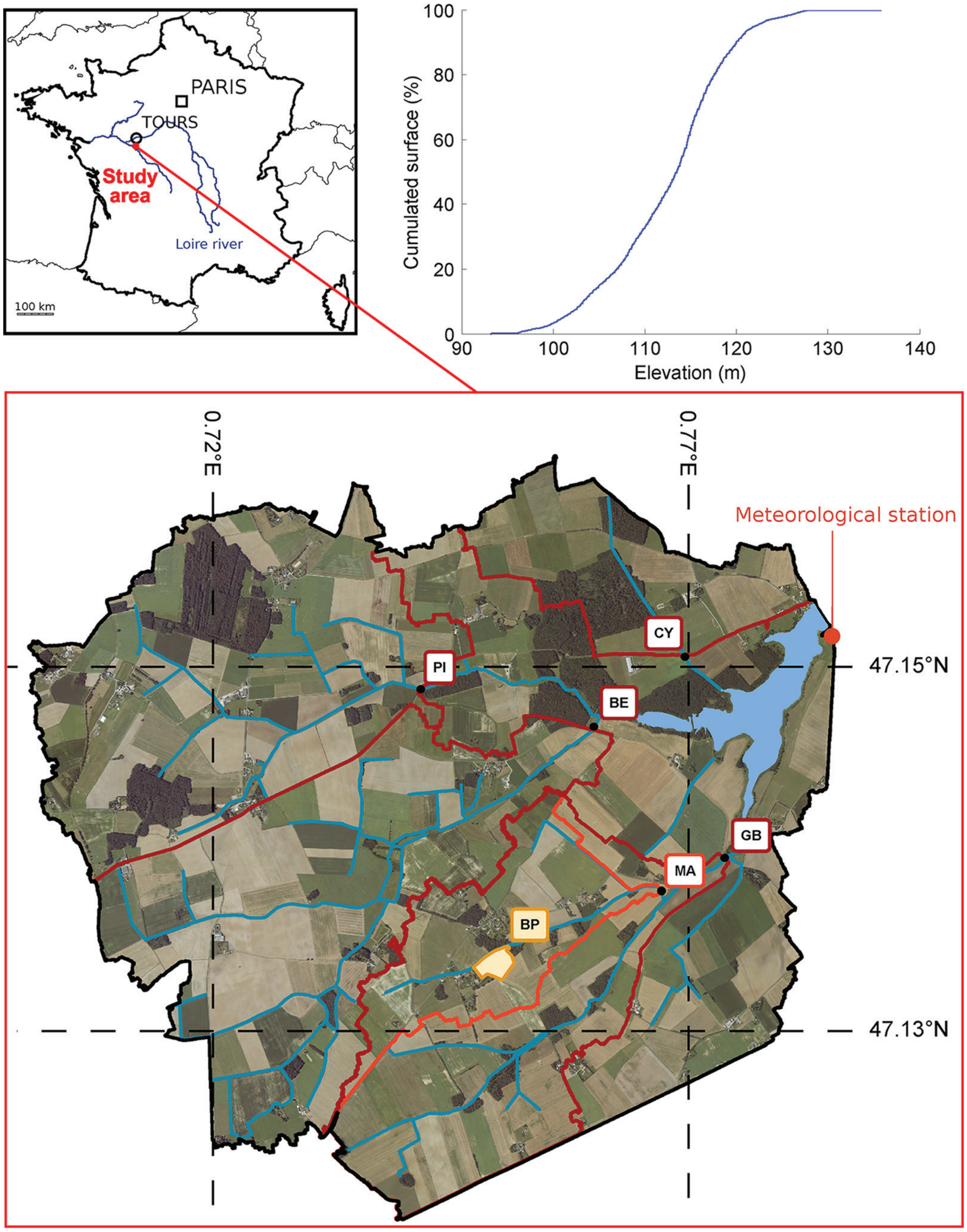

Fig. 1. Location of the Louroux catchment in France, with the monitored subcatchments, and the catchment hypsometric curve. The red dot indicates the location of the meteorological station, and the black dots indicate the monitoring stations (with their respective labels). The dark red lines delineate the different subcatchments: Conteraye (CY), Picarderie (PI), Beaulieu (BE), Masniers (MA), and Grand Bray (GB). The yellow area represents the field connected to the tile drain outlet (Brépinière, BP). Note that this area is embedded within the Masniers subcatchment (light red), which flows into the Grand Bray subcatchment.

Nephelometric sensors were installed at the stations to measure water turbidity. Suspended sediment was sampled in the flow using a Hach-Lange SIGMA SD900 automatic sampler. Sampling was triggered by water level thresholds. The samples were filtered using 0.45 μm filters and oven dried (105°C) to calculate suspended sediment concentrations. These measurements were used to establish a rating curve with the measured turbidity, providing high-frequency measurements of suspended sediment concentrations. Both the water level and the turbidity probes recorded values with a 1-min time step. These very high frequency time series are used to filter out the noise occurring because of episodic probe obstruction (leaves, bubbles, etc.). Accordingly, final datasets were provided with a 15-min resolution. A detailed quantification of the measurement uncertainty was not performed. However, the measurement protocol was similar to that proposed by Navratil et al. (2011). Accordingly, the quantification of the suspended sediment fluxes in the Louroux catchment should be considered with ±20% uncertainties.

A Vantage Pro2 pluviometer was installed close to the catchment outlet and provided rainfall depth measurements with 5-min time steps.

Rainfall and Flood Events Separation

A rainfall event was defined as an event cumulating more than 1 mm. Successive rainfall events were separated by a minimum of 5 h without rainfall, according to a trial-and-error procedure and a visual inspection of the results using values corresponding to the

Table 1. Main topographical and land cover characteristics of the different subcatchments. The elevation difference is the difference between the highest and the lowest points of each subcatchment.

Measurement station	Area	Elevation difference	Ditch network density	Crops	Forest and grassland	Residential areas
	km^2	m	$km\ km^{-2}$	%		
Beaulieu	5.91	25.1	5.7	85	12	3
Conteraye	2.03	14.9	6.2	45	52	3
Grand Bray	5.04	20.9	5.2	88	8	4
Picarderie	5.91	29.1	4.5	55	36	9
Masniers	1.96	20.5	6.9	86	5	9

lag time of the different subcatchments, and comprised between 2 and 6 h. In total, 263 rainfall events were identified. Then, the flood events were extracted as follows: the base flow was calculated for each station according to the method proposed by Chapman (1991), and a runoff threshold (calculated as the difference between total and base-flow discharge) was defined between 0.02 and 0.07 $m^3\ s^{-1}$, with variations between subcatchments. The floods were then associated with rainfall events, starting with the station draining the smallest surface area (Masniers station, 1.96 km^2). A total of 44 storm–flood coupled events were identified at the five monitoring stations.

Statistical Analysis

A statistical analysis was conducted on the flood event characteristics to analyze the processes resulting in water and sediment fluxes measured at the event scale. Water volumes (m^3) and sediment loads (kg) were calculated through the temporal integration of discharge and suspended sediment concentration time series. Different indicators of sediment production and transfer were derived from the field measurements and are described below.

Because rainfall detachment was demonstrated to be a major triggering factor of erosion on hillslopes (e.g., Issa et al., 2006), sediment concentrations ($g\ L^{-1}$) and loads ($t\ km^{-2}$) were analyzed in relationship with various rainfall characteristics. Rainfall maximum intensity ($mm\ h^{-1}$) was selected as an indicator of rainfall detachment because it has been demonstrated to be well correlated with suspended sediment concentration (Cerdan et al., 2002). Moreover, because rainfall kinetic energy (RKE, $J\ m^{-2}\ mm^{-1}$) is increasingly considered as better reflecting rainfall detachment than rainfall intensity (Morgan and Duzant, 2008), it was derived from the maximum rainfall intensity (RI) using the equation proposed by Brandt (1989): $RKE = 8.95 + 8.44 \times \log_{10}(RI)$.

Water discharge ($m^3\ s^{-1}$) was also considered because it integrates all the hydrological processes occurring upstream of the monitoring stations. To discriminate between surface and underground processes, water discharge was subdivided between quick flow and base flow. Peak discharge ($m^3\ s^{-1}$) was used to analyze the effects of instantaneous extreme values on the suspended sediment load at the event scale. Both the mean and maximum values of instantaneous discharge and suspended sediment concentration were also included in the analysis. The peak runoff discharge was deduced from the hydrograph quick flow–base flow separation.

Specific peak discharges ($m^3\ s^{-1}\ km^{-2}$) and water volumes (mm) were calculated to compare the values obtained for the different subcatchments.

Because different hydrograph shapes can result from different processes, other hydrograph characteristics were also calculated, such

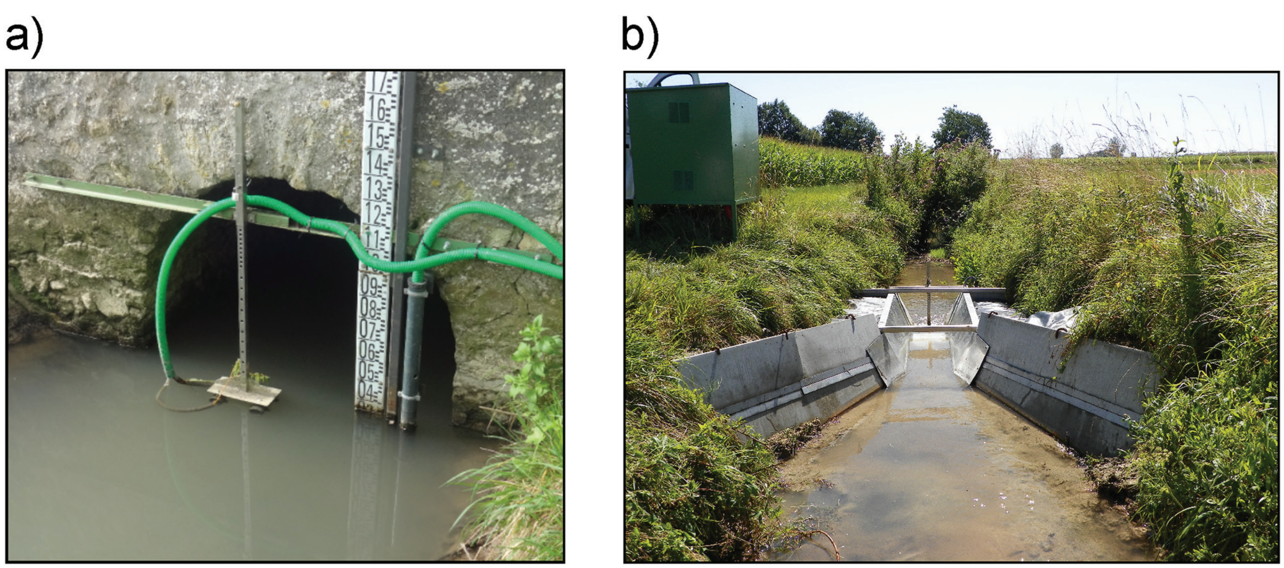

Fig. 2. Typical monitoring station (a) using water level turbidity probe and rating curves in a river (Grand Bray station) and (b) using calibrated flumes (Masniers station).

as the time to peak (s), the recession duration (s), and the timing between rainfall centroid and the peak discharge (s).

Because no preliminary assumption was made on the shape of the different relationships, both Pearson's R and Spearman's ρ were calculated.

Results and Discussion

Hydrological Behavior

A total cumulative rainfall of 1660 mm was measured during the entire monitoring period (2013–2016). The annual rainfall amounted to 641, 548, and 471 mm during these 3 yr, corresponding to 94, 80, and 69%, respectively, of the mean annual rainfall. Accordingly, the monitoring period investigated in this study was considered to be relatively dry. The total rainfall amount varied among seasons: 22% in autumn, 33% in winter, 26% in spring, and 19% in summer.

At the rainfall event scale, rainfall intensity ranged from 2.4 to 60 mm h^{-1} at a 5-min time step. The highest rainfall intensities were recorded during spring: the mean intensity was 21.6 mm h^{-1}, with rainfall events lasting for 8 h on average. During winter, the rainfall events had a mean duration of 9 h and a mean intensity of 11.5 mm h^{-1}.

Among the recorded flood events, 33 occurred during winter, one during autumn, nine during spring, and one during summer. The floods (selected following the procedure described above) contributed to 39 $\pm$ 16% of the annual water fluxes and 79 $\pm$ 9% of the annual sediment fluxes (mean $\pm$ standard deviation across the 3 yr and for the entire set of monitoring stations) and are therefore considered to be representative of the suspended sediment dynamics in this catchment.

The flood event characteristics were very variable, with durations ranging from a few hours to a few days, confirming results obtained in other small headwater catchments (Duvert et al., 2010; Navratil et al., 2011; Sherriff et al., 2015). The hydrographs usually exhibit falling-on-rising-limb duration ratios ranging from 1 (symmetrical hydrographs) to 5 (hydrographs with long falling limbs). Hydrographs with multiple peaks were also recorded, especially during winter when multiple rain events occurred on saturated soils. Accordingly, among the 13 flood events with multiple peaks recorded at the Masniers station, 10 occurred during winter, when the soil was the most likely to be saturated. Runoff coefficients exhibited large variations. For instance, in the Masniers catchment, they ranged from 1 to 34% during the three monitored years. The variations were high both within and between seasons, which is linked to the fact that in these environments flood events can be generated by both saturation and infiltration-excess overland flow (Saffarpour et al., 2016), as well as because of variations in storm characteristics.

Because flow from the tile drains is likely to be observed during periods of high base flow, due to soil column saturation, the percentage of water volume related to quick flow and base flow was calculated during flood events. The base flow proportion exhibited large variations at the flood event scale, representing 36 $\pm$ 9% (mean $\pm$ standard deviation across the different subcatchments) of the flood event volume during winter, 29 $\pm$ 14% in spring, 20 $\pm$ 10% in autumn, and 21 $\pm$ 17% in summer, reflecting the partial contribution of soil saturation to flood generation.

As flood events were more frequent during winter and considering the previous base flow analysis, the measurements demonstrate a vertical connection throughout the soil column, high base flow occurring when the soil was saturated. In this study, flow was recorded in the tile drain during 11.4% of the total monitoring period. This result underlines the need to measure fluxes from tile drains with a high temporal resolution, as initiated in this study. Fluxes measured in the river downstream of the drain station (Masniers) showed that their temporal dynamics were correlated (Fig. 3). Flow in the tile drain was systematically measured during the most significant flood events that occurred at the catchment outlets, when rainfall exceeding 3.4 mm was measured.

In addition, during flood events, the peak discharge at the tile drain station occurred simultaneously (concomitant peaks) or up to 3 h before the peak discharge recorded at the river station (mean time lag of 80 min). Because the river station response integrates both surface runoff and subsurface flow from all the tile-drained fields, this lag reflects the vertical (i.e., movement through the soil column) and lateral (i.e., overland flow and river flow propagation) travel times of water flow. This result demonstrates the significant tile drain contribution to the water fluxes observed in the catchment, as well as their complex behavior. This complexity is associated with the diversity of parameters involved in the

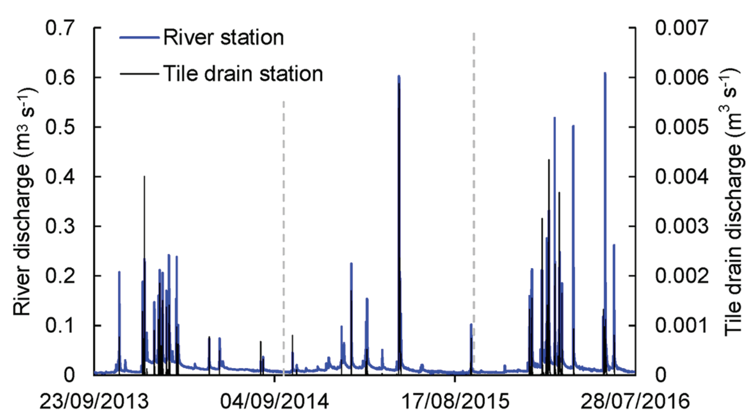

Fig. 3. Tile drain water discharge and corresponding values measured at the river station installed downstream of the drain outlet (i.e., Masniers station). The gray dashed lines indicate the beginning of each hydrological year.

hydrological response of tile drains, which is a function of rainfall, soil type, soil surface state, and crop cultivar (Warsta et al., 2013). Despite the relationship observed between these stations, the specific peak discharge measured at the tile drain station during floods represented 1 to 68% of that recorded at the Masniers river station. Furthermore, there was no clear seasonal distinction, as this contribution reached 23% in winter and 26% in summer. Assuming that the monitored tile drain was representative of those found in the entire catchment, the specific water volume exported from the tile drain would correspond to 10 ± 7.5% (range: 0–44%) of that measured at the Masniers station during flood events. Considering that flow in tile drains occurred exclusively during flood events, with a timing similar to that recorded at the nearby river station, and that it contributed to quick flow, water flow from the tile drains would supply 19 ± 15% (range: 0–59%) of the subcatchment water fluxes and would therefore provide a significant contribution to the water flow transiting the catchment.

Erosion and Suspended Sediment Dynamics

Annual and Event-Scale Dynamics

The specific sediment yields varied between 1 and 38 t km^{-2} yr^{-1}, with strong spatial and temporal variations. These values are comparable to those estimated in similar lowland environments. For instance, Gay et al. (2014) calculated values ranging from 2.9 to 32.4 t km^{-2} yr^{-1} for 111 catchments across the entire Loire River basin (∼10–110,000 km^2). Although these yields remain low compared with those recorded in other environments (e.g., mountainous catchments; Vanmaercke et al., 2011), they may lead to significant environmental problems. This is illustrated by the sediment siltation problem occurring in the pond draining the Louroux catchment (Fig. 1). Foucher et al. (2014) estimated, using estimated deposition rates from sediment coring, that this pond, created during the 11th century, should be completely filled with sediment in about 50 to 100 yr (i.e., during the period from 2050 to 2100).

The temporal analysis of the sediment fluxes revealed that during the selected flood events, the mean contributions of flood events to the annual sediment fluxes was 79 ± 9% and that these fluxes occurred within a mean of 6 d. These results are in agreement with measurements made in other catchments in similar lowland environments (Meybeck et al., 2003). Surprisingly, these findings are also in line with those obtained in other headwater mountainous catchments (Duvert et al., 2010; Navratil et al., 2011). They demonstrate the importance of understanding sediment transfer processes occurring at short timescales in headwater catchments, whatever their physiographic characteristics (e.g., slope distributions). Three main sediment sources were shown to be dominant in these lowland environments (Russell et al., 2001; Walling et al., 2002): channel bank erosion, cropland surface erosion, and transfers from tile drains. In the Louroux catchment, a previous sediment tracing study based on ^{137}Cs measurements demonstrated that cropland surface erosion and/or tile drains supplied most of the sediment to the rivers (Foucher et al., 2015). These findings corroborate those of Uusitalo et al. (2001), although they were made at the plot scale. However, ^{137}Cs measurements did not provide discrimination between cropland surface soil and material transiting tile drains, both exhibiting similar levels of ^{137}Cs, probably because of the migration of very fine particles through the soil column and their export through the tile drainage network.

Processes Governing Sediment Dynamics

For comparable water discharges, and whatever the monitoring station considered, higher sediment concentrations were measured during winter than during spring and summer (Fig. 4), which demonstrates the important seasonality in the erosion and sediment transport behavior of the catchment.

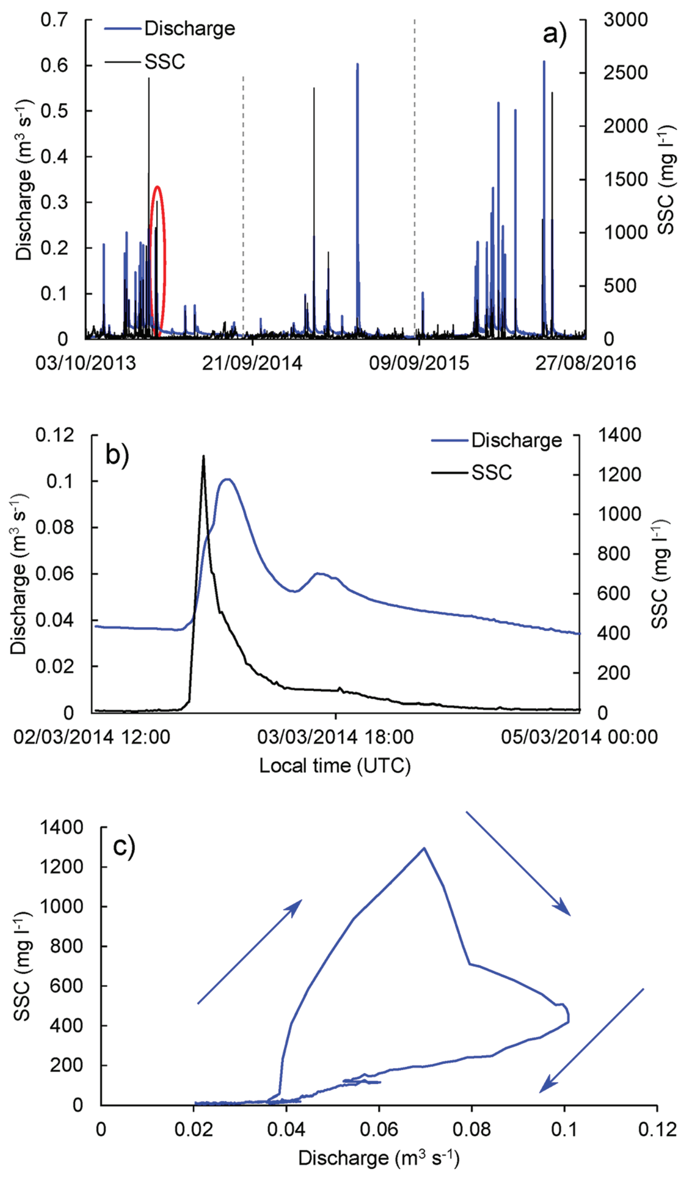

Fig. 4. (a) Discharge and suspended sediment concentration (SSC) at the Masniers station, (b) a close-up of a flood event (indicated by the red circle), and (c) the corresponding SSC–discharge hysteresis relationship. The gray dashed lines in (a) indicate the beginning of each hydrological year.

For the recorded flood events, various patterns were observed in the discharge–suspended sediment concentration relationship. Depending on the monitoring station considered, 67 to 81% of the flood events displayed clockwise hysteresis. The tile drain station mainly displayed (93%) clockwise hysteresis. Only two events displayed concomitant discharge and sediment peaks, and one event displayed an anticlockwise hysteresis. Although the interpretation of clockwise and anticlockwise hysteresis has to be cautious (Duvert et al., 2010; Gao and Josefson, 2012; Kim and Ivanov, 2014; Sherriff et al., 2016), the tile drain station clearly exhibited a different behavior than the other stations. This difference is meaningful because clockwise hysteresis is usually interpreted as reflecting the contribution of a nearby sediment source. In the case of tile drainage, this source can be sediment originating from the soil surface (Foucher et al., 2015) or the remobilization of sediment deposited during a previous flood event.

To get more insight into sediment dynamics in this catchment, the statistical relationships between the variables derived for the five monitoring stations and for all the flood events were analyzed. The tested temporal variables (e.g., time to peak, recession time) did not display significant correlations. These results showed that this small headwater catchment is very reactive at both the flood event and seasonal scales, resulting in a strong variability and a high complexity of the hydrographs. Accordingly, the detailed analysis of the hydrograph across multiple flood events and stations was considered to not be appropriate in the current research. Only integrative variables displayed significant correlation values and are therefore presented in Table 2.

Interestingly, although the relationships between sediment load and rainfall characteristics were weak, the correlation was higher for rainfall cumulative variables than for instantaneous variables. The best relationship was obtained when considering a nonlinear (as reflected by the Spearman coefficient) relationship with cumulative rainfall or a linear (as reflected by the Pearson coefficient) relationship with kinetic energy, which was derived from a power law relationship. These results are in agreement with those of other studies demonstrating that soil detachment is usually described as a power law of rainfall characteristics (Salles et al., 2000). Given the low slopes dominating in the Louroux catchment and that the correlation with rainfall does not explicitly include the transport capacity, it indicates that in lowland environments, the detachment by rainfall is an important actor of erosion and suspended sediment transfers. This result has important implications for designing strategies to limit erosion and sediment transfer problems in similar environments.

The best correlation with the suspended sediment load was obtained with the specific peak discharge (Spearman's $\rho = 0.79$) and was especially good when restricting the analysis to the tile drainage dataset ($\rho = 0.92$).

Tile Drain Dynamics: the Value of High-Frequency Records across Multiple Flood Events

The tile drain station supplied a mean of 13% (range: 0–63%) of the sediment flux transiting the downstream Masniers river station. Although the tile drains displayed a different behavior than the river stations, as demonstrated by the hysteretic pattern analysis, the statistical analysis (Table 2) showed that the main control variable of sediment flux remained the specific peak discharge. For a given specific peak discharge, sediment fluxes from the tile drains overlapped those measured in rivers and were higher on average (Fig. 5).

The similar order of magnitude found at both stations illustrates the significant contribution of tile drains to sediment transiting

Table 2. Values of Pearson (lower part) and Spearman (upper part) correlation coefficients between various hydro-sedimentary variables measured at the four river monitoring stations in the Louroux catchment, France.

Variable†	Vol	Q_{max}	Q_{mean}	SSL	SSC_{max}	SSC_{mean}	RI_{max}	R	RKE	RE
	mm	$m^3 s^{-1} km^{-2}$		$t km^{-2}$	$g L^{-1}$		$mm h^{-1}$	mm	$J m^{-2} mm^{-1}$	$J m^{-2}$
Vol	1	*0.85*‡	*0.78*	*0.83*	0.19	0.22*	0.12	0.51*	0.12	0.35*
Q_{max}	*0.70*	1	*0.94*	0.79*	0.25*	0.31*	0.19*	0.52*	0.19*	0.40*
Q_{mean}	*0.68*	*0.94*	1	0.68*	0.11	0.28*	0.16*	0.41*	0.16	0.32*
SSL	*0.67*	0.49*	0.43*	1	0.61*	0.65*	0.21	0.43*	0.21*	0.36*
SSC_{max}	0.12	0.17*	0.10	0.48	1	*0.84*	0.27	0.16*	0.27*	0.24*
SSC_{mean}	0.17*	0.22*	0.20	0.61*	*0.71*	1	0.17*	0.03	0.17	0.12*
RI_{max}	0.17	0.23*	0.16	0.33*	0.33	0.20	1	*0.48*	*1*	*0.78*
R	0.53*	0.60*	0.52	0.32*	0.14*	0	*0.46*	1	*1*	*0.84*
RKE	0.12	0.18*	0.12	0.23	0.24	0.14	*0.92*	*0.38*	1	*0.77*
RE	0.31*	0.31*	0.27	0.44*	0.36	0.19	*0.79*	*0.70*	*0.69*	1

* Significant at $p < 0.05$.
† Vol, total water volume normalized by the catchment surface; Q, specific discharge; SSL, specific suspended sediment load; SSC, suspended sediment concentration; RI_{max}, maximum rainfall intensity; R, cumulative rainfall during the rainfall event; RKE, maximum rainfall kinetic energy flux; RE, total rainfall energy during the rainfall event.
‡ Auto-correlated variables are indicated in italics; significance is reported for variables that are not auto-correlated.

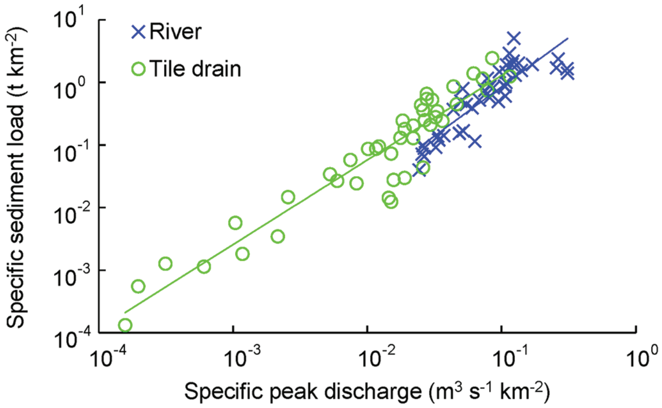

Fig. 5. Relationship between specific sediment loads and specific peak discharges for the flood events recorded at the tile drain station and the downstream Masniers river station.

the rivers in this catchment. On average, specific sediment fluxes measured in rivers at comparable specific peak discharges are 53% lower than those measured at tile drain outlets. This probably results from sediment deposition and storage in the channel network. For the higher peak discharges, the higher transport capacity of the flow resulted in limited deposition in the ditches and led to the remobilization of the material deposited on the channel bed. Accordingly, the two regressions converged toward similar suspended sediment loads at high specific peak discharges.

Given the high correlation observed between the specific peak discharge and the water volume and the low correlation between the specific peak discharge and sediment concentrations (Table 2), the water volume infiltrating the tile drain network should control sediment exports that are well correlated to the specific peak discharge. This finding improves our understanding of the sediment dynamics in tile drainage networks. Particles from the soil in contact with the tiles preferentially fall into them and are then transported through drains. Foucher et al. (2015) showed that these particles are tagged with ^{137}Cs, which demonstrates that these particles originate from the tilled layer of the soil.

Although the specific sediment load increased with the specific peak discharge, these integrative variables mask a strong temporal variability. The high-frequency measurements made at the tile drain outlet (Fig. 6) remained comparable with the very few data found in the literature (Turtola et al., 2007; Warsta et al., 2014). They were therefore used to compare the tile drain sediment dynamics with those found at the downstream Masniers monitoring station.

A sediment dilution effect was observed at the tile drain station, with the measurement of maximum suspended sediment concentrations during the lowest discharges. Furthermore, high suspended sediment concentrations were never measured during high discharge periods. This result probably reflects that the mass of very fine particles that is in suspension in overland flow during rainfall events at the soil surface and that may migrate through the soil pores remained constant regardless of the rainfall characteristics. Accordingly, an almost constant mass of detached fine particles transited the tile drains regardless of the water volume available for percolation. Sediments can also deposit in the tile drainage network at the end of the major flood events. They will then be preferentially flushed at the beginning of subsequent flood events, which is consistent with the dominance of clockwise hysteresis and the decreasing sediment concentrations throughout events found at the tile drain station.

During flood events, the suspended sediment concentrations measured at the tile drain outlet and at the downstream Masniers monitoring station remained comparable, although the river station exhibited generally lower concentrations: the first, second (median), and ninth deciles were 2, 25, and 250 mg L^{-1}, respectively, at the tile drain station vs. 8, 29, and 194 mg L^{-1}, respectively, at the river station. However, the highest concentrations were measured in the river during the most intense flood event: the

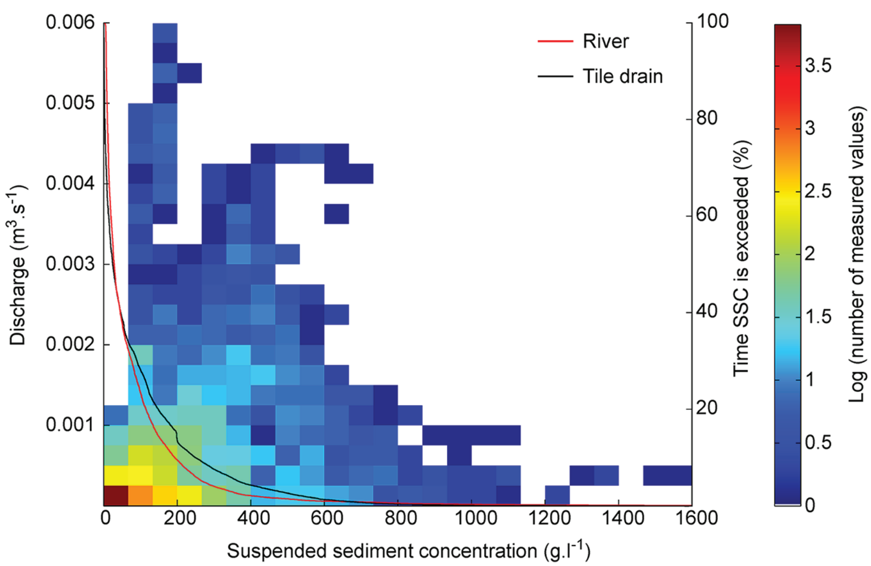

Fig. 6. Relationship between measured suspended sediment concentration and water discharge at the tile drain station (Brépinière). The color map indicates the number of records during flood events (logarithmic scale). The black and red lines (secondary *y* axis) indicate the percentage of monitoring time when the suspended sediment concentration (SSC) was exceeded at the tile drain station and at the downstream station (Masniers), respectively.

maximum recorded value was 2500 mg L^{-1}. Such high concentrations measured in the river compared with the tile drain reflected the particularly large transport capacity of the river and the remobilization of particles from the channel bed during that event.

An Overview of the Catchment Sediment Dynamics

From the results of the statistical analysis, the relationship between specific peak discharges and suspended sediment loads was analyzed to further characterize sediment dynamics at the catchment scale (Fig. 7). Because the relationship was demonstrated not to be linear (Table 2), the regressions were established using nonlinear least square regressions (Asselman, 2000).

Values deduced from the regressions of the relationships between the maximum specific discharge and the specific suspended sediment load (Q_{max}–SSL) for the different subcatchment outlets were compared with those found in the literature. Duvert et al. (2012) analyzed sediment yield from eight headwater catchments located in France, Mexico, and Spain. These catchments varied in size, land use, and slope gradient. However, the studied catchments were mostly mountainous and did not include lowland environments. In their study, values of the exponent of the Q_{max}–SSL relationship were found to vary from 0.9 to 1.9, reflecting changes in antecedent soil moisture conditions, sediment storage, and remobilization on hillslopes and in the channel, as well as physiographic factors (e.g., hillslope gradient, river longitudinal gradient). In our study, values varied from 1.1 to 1.6 and therefore remained in the same range, indicating that the low Strahler order of the river (corresponding to headwater catchments) largely controls this relationship. These results also suggest that the catchment physiographic characteristics do not control to a large extent the variations of this exponent, which have important implications to understand sediment fluxes in headwater catchments and to design effective remediation strategies. This is confirmed by the similar regression values obtained for the various Louroux subcatchments characterized by a dominance of cropland (Fig. 7a).

Accordingly, the mean behavior of the Louroux catchment should be independent of the spatial heterogeneities observed in the cultivated subcatchments (e.g., local slope variations, spatial crop distributions). In contrast, a different behavior was observed in the Conteraye subcatchment characterized by the highest grassland and forest cover proportions (Table 1) and the absence of tile drains. Sediment yields at Conteraye varied from 1 to 4 t km^{-2} yr^{-1}, whereas they oscillated from 7 to 38 t km^{-2} yr^{-1} at the other stations. This result confirmed that land use is the primary factor controlling the sediment response of the subcatchments.

Although the results of regression analyses were very similar among subcatchments, dispersion was observed around their mean behavior, with determination coefficients ranging from $R^2 = 0.31$ (Grand Bray catchment) to $R^2 = 0.75$ (Masniers catchment), indicating that this relationship varied with time. The analysis of the temporal dynamics (Fig. 7b) revealed that the highest sediment fluxes occurred in winter. Because this period is characterized by soil saturation, antecedent moisture conditions and sediment availability should exert an important control on suspended sediment load variations. These results confirm those obtained by Le Gall et al. (2017), who compared fallout radionuclide (including ^{7}Be and ^{137}Cs) concentrations measured in sediment collected in ephemeral flow on hillslopes and in the rivers of the Louroux catchment. They demonstrated that large sediment stocks (depleted in ^{7}Be) were available in the channel at the beginning of the hydrological year and that they were progressively washed off during flood events in winter. Then, in spring, sediment recently eroded from the hillslopes (enriched in both ^{7}Be and ^{137}Cs) provided the dominant (80 ± 20%) source of material transiting the rivers, with an estimated residence time of 20 ± 5 d. This hypothesis of stock-limited transfer would explain the limited dispersion in the specific peak discharge–sediment load in winter. Because large stocks of sediment were available in the river channel at the beginning of winter, sediment fluxes were transport limited. The small dispersion of values in the relationship ($R^2 = 0.80$) result from limited restrictions on sediment export, with a high transport capacity and a high sediment availability, as reflected by an

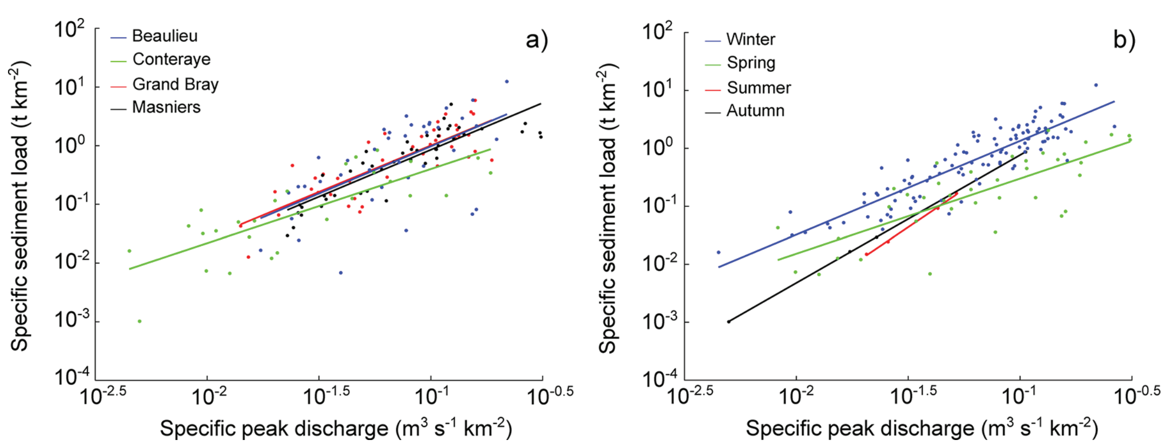

Fig. 7. Regressions established between specific peak discharges and specific sediment loads, when considering (a) the different river monitoring stations and (b) the season of the flood occurrence. Bi-logarithmic axes were used given the large variability of the measured values.

increase of the specific sediment load with specific peak discharges. This abundant sediment stock probably accumulated during spring and summer, when water discharge and sediment export were low because of the high infiltration occurring in cropland densely covered by vegetation during this period. Moreover, the maximum rainfall intensity recorded at a 5-min time step was higher in spring (mean: 21.6 mm h^{-1}) than winter (11.5 mm h^{-1}). Although this higher rainfall intensity may have resulted in higher sediment fluxes in spring (Cerdan et al., 2002), the corresponding fluxes measured in the river were lower. The higher rainfall intensities recorded in spring may have generated a sediment stock on hillslopes, as reflected by the non-negligible correlations of sediment load with rainfall-related variables (Table 2). The extensive deposition of sediment that was required to generate this significant stock explains the higher dispersion observed in spring ($R^2 = 0.61$) than in winter: an increase in specific peak discharge did not necessarily generate an increase in specific sediment flux because of the limited availability of sediment material. Although this process was already identified by Le Gall et al. (2017) using fallout radionuclide measurements, our study quantified for the first time the impacts of the sediment stock availability in the river channel through regression analysis.

The role of tile drains in sediment transfers at the catchment scale was also clarified in this study. Higher sediment concentrations were generally measured at the tile drain outlet than the river stations, which is hypothesized to reflect the direct transfer of sediment through the drains while significant deposition may occur in river channels (except during the most intense floods). Our results corroborate those obtained at the field scale, where Turtola et al. (2007) measured 37 to 94% of the annual soil loss transported by subsurface flow rather than by overland flow. Our study showed that these results also apply at the catchment scale. Drains should therefore be explicitly taken into account in monitoring schemes when investigating sediment production and transport in similar lowland agricultural catchments.

Conclusions

An agricultural drained catchment of central France representative of those found in the middle Loire River basin was equipped with five hydro-sedimentary monitoring stations to supplement the lack of sediment measurements available in these environments. Forty-four flood events were recorded between 2013 and 2016, mostly during winter (33 events) and spring (nine events). Our results demonstrated the complex behavior of these catchments, characterized by the occurrence of both infiltration-excess overland flow and saturation runoff.

Specific sediment yields varied between 1 and 38 t km^{-2} yr^{-1}, and 79 ± 9% of the sediment fluxes occurred during flood events. At the flood event scale, a good nonlinear statistical relationship was found between the specific sediment load and the specific peak discharge. The catchment Strahler's order was shown to control variations in this relationship and the suspended sediment load. Land use was confirmed to be the dominant factor controlling sediment flux variations among subcatchments. The significance of antecedent soil moisture and the availability of a sediment stock in the channel for remobilization during flood events were also shown to be of prior importance. In contrast, the subcatchment physiographic properties were shown to be of minor importance.

Flow in tile drains was shown to be very episodic. However, they exported significant sediment fluxes, comparable to or even higher (mean of 53%) than those measured at the river downstream station. Accordingly, tile drainage is shown to be a significant process to consider when investigating sediment transfer in lowland agricultural catchments. Future work should therefore further analyze and quantify sediment deposition processes and the temporal evolution of a potential available stock of sediment in the river network in these environments.

Acknowledgments

This work received financial support from the Loire-Brittany Water Agency (in the framework of the Tracksed and Drastic research projects, under the close supervision of Xavier Bourrain, Jean-Noël Gauthier, and Anne Colmar). We would like to acknowledge the landowners who granted access to their fields for the installation of the monitoring stations: Mr. Chaumont, Destouches, Gaudron, Gault, Maingault, Legros, and Le Men. The technical assistance of Aurélia Matthieu, Gaëtane Chirié, and Jean-Paul Bakyono as well as the work of Laura Boennec and Safiya Cisse is gratefully acknowledged.

References

Asselman, N.E.M. 2000. Fitting and interpretation of sediment rating curves. J. Hydrol. 234:228–248. doi:10.1016/S0022-1694(00)00253-5

Auerswald, K., P. Fiener, and R. Dikau. 2009. Rates of sheet and rill erosion in Germany: A meta-analysis. Geomorphology 111:182–193. doi:10.1016/j.geomorph.2009.04.018

Bradford, J.M., J.E. Ferris, and P.A. Remley. 1987. Interrill soil erosion processes: II. Relationship of splash detachment to soil properties. Soil Sci. Soc. Am. J. 51:1571–1575. doi:10.2136/sssaj1987.03615995005100060030x

Brandt, C.J. 1989. The size distribution of throughfall drops under vegetation canopies. Catena 16:507–524. doi:10.1016/0341-8162(89)90032-5

Bilotta, G.S., R.E. Brazier, P.M. Haygarth, C.J.A. Macleod, P. Butler, S. Granger, et al. 2008. Rethinking the contribution of drained and undrained grasslands to sediment-related water quality problems. J. Environ. Qual. 37:906–914. doi:10.2134/jeq2007.0457

Cea, L., C. Legout, T. Grangeon, and G. Nord. 2016. Impact of model simplifications on soil erosion predictions: Application of the GLUE methodology to a distributed event-based model at the hillslope scale. Hydrol. Processes 30:1096–1113. doi:10.1002/hyp.10697

Cerdan, O., Y. Le Bissonnais, V. Souchère, P. Martin, and V. Lecomte. 2002. Sediment concentration in interrill flow: Interactions between soil surface conditions, vegetation and rainfall. Earth Surf. Processes Landforms 27:193–205. doi:10.1002/esp.314

Chapman, T.G. 1991. Comment on "Evaluation of automated techniques for base flow and recession analyses" by R.J. Nathan and T.A. McMahon. Water Resour. Res. 27:1783–1784. doi:10.1029/91WR01007

Delmas, M., O. Cerdan, B. Cheviron, J.M. Mouchel, and F. Eyrolle. 2012. Sediment export from French rivers to the sea. Earth Surf. Processes Landforms 37:754–762.

de Vente, J., and J. Poesen. 2005. Predicting soil erosion and sediment yield at the basin scale: Scale issues and semi-quantitative models. Earth Sci. Rev. 71:95–125. doi:10.1016/j.earscirev.2005.02.002

Duvert, C., N. Gratiot, O. Evrard, O. Navratil, J. Némery, C. Prat, and M. Esteves. 2010. Drivers of erosion and suspended sediment transport in three headwater catchments of the Mexican central highlands. Geomorphology 123:243–256. doi:10.1016/j.geomorph.2010.07.016

Duvert, C., G. Nord, N. Gratiot, O. Navratil, E. Nadal-Romero, N. Mathys, J. Némery, et al. 2012. Towards prediction of suspended sediment yield from peak discharge in small erodible mountainous catchments (0.45–22 km^2) of France, Mexico and Spain. J. Hydrol. 454–455:42–55. doi:10.1016/j.jhydrol.2012.05.048

Foucher, A., P.J. Laceby, S. Salvador-Blanes, O. Evrard, M. Le Gall, I. Lefevre, et al. 2015. Quantifying the dominant sources of sediment in a drained lowland agricultural catchment: The application of a thorium-based particle size correction in sediment fingerprinting. Geomorphology 250:271–281. doi:10.1016/j.geomorph.2015.09.007

Foucher, A., S. Salvador-Blanes, O. Evrard, A. Simmoneau, E. Chapron, T. Courp, et al. 2014. Increase in soil erosion after agricultural intensification: Evidence from a lowland basin in France. Anthropocene 7:30–41. doi:10.1016/j.ancene.2015.02.001

Gao, P., and M. Josefson. 2012. Event-based suspended sediment dynamics in a central New York watershed. Geomorphology 139–140:425–437. doi:10.1016/j.geomorph.2011.11.007

García-Ruiz, J.M., E. Nadal-Romero, N. Lana-Renault, and S. Berguería. 2013. Erosion in Mediterranean landscapes: Changes and future challenges. Geomorphology 198:20–36. doi:10.1016/j.geomorph.2013.05.023

Gay, A., O. Cerdan, M. Delmas, and M. Desmet. 2014. Variability of suspended sediment yields within the Loire river basin (France). J. Hydrol. 519:1225–1237. doi:10.1016/j.jhydrol.2014.08.045

Hairsine, P.B., and C.W. Rose. 1992. Modeling water erosion due to overlandflow using physical principles: 1. Sheet flow. Water Resour. Res. 28:237–243. doi:10.1029/91WR02380

Issa, O.M., Y. Le Bissonnais, O. Planchon, D. Favis-Mortlock, N. Silvera, and J. Wainwright. 2006. Soil detachment and transport on field- and laboratory-scale interrill areas: Erosion processes and the size-selectivity of eroded sediment. Earth Surf. Processes Landforms 31:929–939. doi:10.1002/esp.1303

Jomaa, S., D.A. Barry, A. Brovelli, G.C. Sander, J.-Y. Parlange, B.C.P. Heng, and H.J. Tromp-Van Meerveld. 2010. Effect of raindrop splash transversal width on soil erosion: Laboratory flume experiments and analysis with the Hairsine–Rose model. J. Hydrol. 395:117–132. doi:10.1016/j.jhydrol.2010.10.021

Kemp P., D. Sear, A. Collins, P. Naden, and I. Jones. 2011. The impacts of fine sediment on riverine fish. Hydrol. Processes 25:1800–1821. doi:10.1002/hyp.7940

Kim, J., and V. Ivanov. 2014. On the nonuniqueness of sediment yield at the catchment scale: The effects of soil antecedent conditions and surface shield. Water Resour. Res. 50:1025–1045. doi:10.1002/2013WR014580

King, K.W., N.R. Fausey, and M.R. Williams. 2014. Effects of subsurface drainage on streamflow in an agricultural headwater watershed. J. Hydrol. 519:438–445. doi:10.1016/j.jhydrol.2014.07.035

Kinnell, P.I.A. 2005. Raindrop-impact-induced erosion processes and prediction: A review. Hydrol. Processes 19:2815–2844. doi:10.1002/hyp.5788

Kjelland, M., C. Woodley, T. Swannack, and D. Smith. 2015. A review of the potential effects of suspended sediment on fishes: Potential dredging-related physiological, behavioral, and transgenerational implications. Environ. Syst. Decisions 35:334–350. doi:10.1007/s10669-015-9557-2

Le Bissonnais, Y., and M.J. Singer. 1992. Crusting, runoff, and erosion response to soil-water content and successive rainfalls. Soil Sci. Soc. Am. J. 56:1898–1903. doi:10.2136/sssaj1992.03615995005600060042x

Le Gall, M., O. Evrard, A. Foucher, J.P. Laceby, S. Salvador-Blanes, L. Maniere, et al. 2017. Investigating the temporal dynamics of suspended sediment during flood events with ^{7}Be and $^{210}Pb_{xs}$ measurements in a drained lowland catchment. Sci. Rep. 7:42099. doi:10.1038/srep42099

Li, H., M. Sivapalan, F. Tian, and D. Liu. 2010. Water and nutrient balances in a large tile-drained agricultural catchment. Hydrol. Earth Syst. Sci. 14:2259–2275. doi:10.5194/hess-14-2259-2010

López-Vicente, M., L. Quijano, L. Palazón, and L. Gaspar. 2015. Assessment of soil redistribution at catchment scale by coupling a soil erosion model and a sediment connectivity index (central Spanish pre-Pyrenees). Cuad. Invest. Geogr. 41:127–147.

Macrae, M.L., M.C. English, S.L. Schiff, and M. Stone. 2007. Intra-annual variability in the contribution of tile drains to basin discharge and phosphorous export in a first-order agricultural catchment. Agric. Water Manage. 92:171–182. doi:10.1016/j.agwat.2007.05.015

Meybeck, M., L. Laroche, H.H. Dürr, and J.P.M. Syvitski. 2003. Global variability of daily total suspended solids and their fluxes in rivers. Global Planet. Change 39:65–93. doi:10.1016/S0921-8181(03)00018-3

Milliman, J.D., and P.M. Syvitski. 1992. Geomorphic/tectonic control of sediment discharge to the ocean: The importance of small mountainous rivers. J. Geol. 100:525–544. doi:10.1086/629606

Morgan, R.P.C., and J.H. Duzant. 2008. Modified MMF (Morgan–Morgan–Finney) model for evaluating effects of crops and vegetation cover on soil erosion. Earth Surf. Processes Landforms 33:90–106. doi:10.1002/esp.1530

Muma, M., A.N. Rouseau, and S.J. Gumiere. 2016. Assessment of the impact of subsurface agricultural drainage on soil water storage and flows of a small watershed. Water 8(8):326. doi:10.3390/w8080326

Navratil, O., M. Esteves, C. Legout, N. Gratiot, J. Némery, S. Willmore, and T. Grangeon. 2011. Global uncertainty analysis of suspended sediment monitoring using turbidimeter in a small mountainous river catchment. J. Hydrol. 398:246–259. doi:10.1016/j.jhydrol.2010.12.025

Nord, G., and M. Esteves. 2005. A physically based model of erosion processes at the plot scale. Water Resour. Res. 41:W08407. doi:10.1029/2004WR003690

Owens, P.N., R.J. Batalla, A.J. Collins, B. Gomez, D.M. Hicks, A.J. Horowitz, et al. 2005. Fine-grained sediment in river systems: Environmental significance and management issues. River Res. Appl. 21:693–717. doi:10.1002/rra.878

Parsons, A.J., L. Bracken, R.E. Poeppl, J. Wainwright, and S.D. Keesstra. 2015. Introduction to special issue on connectivity in water and sediment dynamics. Earth Surf. Processes Landforms 40(9):1275–1277. doi:10.1002/esp.3714

Rasplus, L., J.J. Macaire, and G. Alcaydé. 1982. Carte géologique de Bléré au 1:5000. Bureau de Recherches Géologiques et Minières, Orléans, France.

Rozemeijer, J.C., Y. van der Velde, F.C. van Geer, M.F.P. Bierkens, and H.P. Broers. 2010. Direct measurements of the tile drain and groundwater flow route contributions to surface water contamination: From field-scale concentration patterns in groundwater to catchment-scale surface water quality. Environ. Pollut. 158:3571–3579. doi:10.1016/j.envpol.2010.08.014

Russell, M.A., D.E. Walling, and R.A. Hodgkinson. 2001. Suspended sediment sources in two small lowland agricultural catchments in the UK. J. Hydrol. 252:1–24. doi:10.1016/S0022-1694(01)00388-2

Saffarpour, S., A.W. Western, R. Adams, and J.J. McDonnell. 2016. Multiple runoff processes and multiple thresholds control agricultural runoff generation. Hydrol. Earth Syst. Sci. 20:4525–4545. doi:10.5194/hess-20-4525-2016

Salles, C., J. Poesen, and F. Govers. 2000. Statistical and physical analysis of soil detachment by raindrop impact: Rain erosivity and threshold energy. Water Resour. Res. 36:2721–2729. doi:10.1029/2000WR900024

Sherriff, S.C., J.S. Rowan, O. Fenton, P. Jordan, A.R. Melland, P.E. Mellander, and D.O. Huallachain. 2016. Storm event suspended sediment-discharge hysteresis and controls in agricultural watersheds: Implications for watershed scale sediment management. Environ. Sci. Technol. 50:1769–1778. doi:10.1021/acs.est.5b04573

Sherriff, S.C., J.S. Rowan, A.R. Melland, P. Jordan, O. Fenton, and D.O. Huallachain. 2015. Investigating suspended sediment dynamics in contrasting agricultural catchments using ex situ turbidity-based suspended sediment monitoring. Hydrol. Earth Syst. Sci. 19:3349–3363. doi:10.5194/hess-19-3349-2015

Smith, H.G., and W.H. Blake. 2014. Sediment fingerprinting in agricultural catchments: A critical re-examination of source discrimination and data corrections. Geomorphology 204:177–191. doi:10.1016/j.geomorph.2013.08.003

Turtola, E., L. Alakuku, R. Uusitalo, and A. Kaseva. 2007. Surface runoff, subsurface drainflow and soil erosion as affected by tillage in a clayey Finnish soil. Agric. Food Sci. 16:332–351. doi:10.2137/145960607784125429

Ulén, B., and K. Persson. 1999. Field-scale phosphorous losses from a drained clay soil in Sweden. Hydrol. Processes 13:2801–2812. doi:10.1002/(SICI)1099-1085(19991215)13:17<2801::AID-HYP900>3.0.CO;2-G

Uusitalo, R., E. Turtola, T. Kauppila, and T. Lilja. 2001. Particulate phosphorous and sediment in surface runoff and drainflow from clayey soils. J. Environ. Qual. 30:589–595. doi:10.2134/jeq2001.302589x

Vanmaercke, M., J. Poesen, G. Verstraeten, J. de Vente, and F. Ocakoglu. 2011. Sediment yield in Europe: Spatial patterns and scale dependency. Geomorphology 79:72–92.

Wainwright, J., A.J. Parsons, E.N. Müller, R.E. Brazier, D.M. Powell, and B. Fenti. 2008. A transport-distance approach to scaling erosion rates: I. Background and model development. Earth Surf. Processes Landforms 33:813–826. doi:10.1002/esp.1624

Walling, D.E., and A.L. Collins. 2008. The catchment sediment budget as a management tool. Environ. Sci. Policy 11:136–143. doi:10.1016/j.envsci.2007.10.004

Walling, D.E., M.A. Russell, R.A. Hodgkinson, and Y. Zhang. 2002. Establishing sediment budgets for two small lowland agricultural catchments in the UK. Catena 47:323–353. doi:10.1016/S0341-8162(01)00187-4

Warsta L., A. Taskinen, H. Koivusalo, M. Paasonen-Kivekäs, and T. Karvonen. 2013. Modelling soil erosion in a clayey, subsurface-drained agricultural field with a three-dimensional FLUSH model. J. Hydrol. 498:132–143. doi:10.1016/j.jhydrol.2013.06.020

Warsta, L., A. Taskinen, M. Paasonen-Kivekäs, T. Karvonen, and H. Koivusalo. 2014. Spatially distributed simulation of water balance and sediment transport in an agricultural field. Soil Tillage Res. 143:26–37. doi:10.1016/j.still.2014.05.008